Pseudomorphic to orthomorphic growth of Fe films on $Cu_3Au(001)$

F. Bruno,[1] S. Terreni,[2] L. Floreano,[1] A. Cossaro,[1] D. Cvetko,[1,3] P. Luches,[4] L. Mattera,[2] A. Morgante,[1,5]
R. Moroni,[2] M. Repetto,[2] A. Verdini,[1] and M. Canepa[2,*]
[1]*Laboratorio TASC dell'Istituto Nazionale per la Fisica della Materia, Trieste, Italy*
[2]*INFM and Dipartimento di Fisica, Università di Genova, via Dodecaneso 33, I-16146 Genova, Italy*
[3]*Department of Physics, University of Ljubljana, Slovenia, and Sincrotrone Trieste, Italy*
[4]*INFM and Dipartimento di Fisica, Università di Modena e Reggio Emilia, Modena, Italy*
[5]*Dipartimento di Fisica dell'Università di Trieste, Italy*
(Received 21 March 2001; revised manuscript received 19 April 2002; published 28 June 2002)

The structure of Fe films grown on the (001) surface of a Cu_3Au single crystal at room temperature has been investigated by means of grazing incidence x-ray diffraction (GIXRD) and photo/Auger–electron diffraction (ED) as a function of thickness in the (3–36)-Å range. The combination of GIXRD and ED allows one to obtain quantitative information on the in-plane spacing *a* from the former technique, and the ratio between the vertical spacing *c* and *a*, from the latter one. At low coverage the film grows pseudomorphic to the face-centered-cubic substrate. The experimental results obtained on a film of 8 Å thickness clearly indicate the overcoming of the limit for pseudomorphic growth. Above this limit the film is characterized by the coexistence of the pseudomorphic phase with another tetragonally strained phase γ, which falls on the epitaxial line of ferromagnetic face-centered cubic Fe. Finally, the development of a body-centered phase α, whose unit cell is rotated by 45° with respect to the substrate one, has been clearly observed at ~17 Å. α is the dominating phase for film thickness above ~25 Å and its lattice constant evolves towards the orthomorphic phase in strict quantitative agreement with epitaxial curves calculated for body-centered tetragonal iron phases.

DOI: 10.1103/PhysRevB.66.045402 PACS number(s): 68.55.−a, 68.55.Jk, 61.14.Qp

I. INTRODUCTION

Very thin iron films, with physical properties at variance with the ordinary α-Fe phase, can be grown on appropriately chosen substrates.[1] Such ''artificial'' phases represent an ideal ground in the investigation of the interplay between the structure and the magnetic properties of materials.[2] In this field, the $Cu_3Au(001)$ surface has been considered as a candidate for the stabilization of a face-centered cubic (fcc), expanded volume, high-spin Fe phase.[3] For this substrate, a model of the so-called epitaxial lines of iron, calculated within the frame of linear elasticity theory, suggested the formation of a tetragonally strained phase, with some uncertainty on its body- or face-centered geometry.[4] The calculations did not consider interdiffusion processes between the Fe deposit and surface atoms, but both intermixing at the interface and substrate segregation have been reported for Fe deposited at room temperature (RT) on Cu(001) (Ref. 5) and on Au(001).[6,7]

In previous research on the magnetism of the $Fe/Cu_3Au(001)$ films, three regions of thickness of different properties were identified.[8–10] At submonolayer coverage no hysteresis loops were detected. A second region was instead characterized by a magnetization perpendicular to the surface. Then, at a critical thickness Θ_{sw} of the order of a few monolayers and depending on the temperature of deposition, the magnetization was found to switch to an in-plane orientation [spin reorientation (SRO) transition] as in ordinary α-Fe.

In spite of an overall agreement on film magnetism, no general consensus has been reached about the film structure. Regarding RT growth, an early low-energy electron-diffraction (LEED) study claimed the occurrence of a face-centered cubic phase up to 7 monolayers (ML).[8] In a more recent LEED I-V investigation the SRO transition (Θ_{sw} ~4 ML) was tightly related to a transition from an fcc to a bcc-like phase;[9] the LEED analysis was successively backed by a scanning tunnel microscope study in the coverage range of the SRO transition, pointing out a complex topography assigned to the coexistence of different phases.[11] Another LEED I-V study, backed by dynamical calculations, proposed instead a body-centered-tetragonal (bct) structure down to $\Theta = 3.3$ ML with no apparent correlation between structural properties and the SRO transition.[12] In fact, the latter experiments must be carefully taken into consideration, since they were performed on substrates prepared by predepositing 2 ML of Fe at 150 K. For this temperature and thickness range, we have recently shown that the structure and morphology of the growing film is driven by electronic mechanisms,[13] whereas only strain and thermally activated processes drive the RT growth. Finally, in a recent electron-scattering experiment [in the so-called primary-beam diffraction modulated electron emission configuration (PDMEE)] (Ref. 14) an fcc-like structure was found for $\Theta < 4$ ML; then in a region extending up to ≈23 ML, two different phases were detected. A unique phase of bct-type was finally detected, at least within the outermost layers, for relatively thicker films, in agreement with results of Ref. 12. Reference 14 considered atomic exchange processes in some details, indicating the occurrence of a limited Au intermixing and segregation at the initial stages of growth.

The somewhat conflicting results demand for further investigation. Here we report on experiments of $Fe/Cu_3Au(001)$ RT growth performed at the ALOISA

beamline at the Elettra Synchrotron (Trieste, Italy).[15] Our investigation deals with a structural characterization of films in a thickness range of 3–36 Å, performed by means of x-ray induced photo- (and/or Auger-) electron diffraction (from now on ED for brevity) in the so-called forward-scattering condition. In this condition, the emission intensity is enhanced along the direction of interatomic axes by means of a focusing effect.[16] The angular position of focusing peaks in polar ED scans is well known to provide ''simple,'' chemically selected, short-range information on the structure of the topmost layers of the films.[17,18] Furthermore, the availability of reliable calculations codes allows for a close comparison with experimental data and for quantitative analysis.[19]

In our experimental approach,[20] ED data are backed by grazing incidence x-rays diffraction (GIXRD) measurements, supplying information about the in-plane lattice parameter of films[21] and about the film morphology. In the following section details on the experimental procedures are reported. Experimental data will be described in Sec. III A, quantitative analysis of the data can be found in the Sec. IV A discussion of the results obtained follows in Sec. V A, and the conclusions can be found in Sec. VI.

II. EXPERIMENT

The beamline ALOISA allows users to perform both electron spectroscopy and x-ray surface diffraction measurements under the same experimental conditions.[15,22] The sample is mounted on a six-degrees-of-freedom manipulator, specially designed to select with great accuracy (0.01°) the grazing angle of the beam electric field. The temperature of the sample, measured by thermocouples, can be varied by resistive heating and liquid-nitrogen cooling. The UHV experimental chamber (base pressure in the 10^{-11}-mbars range) hosts the hemispherical electron analyzers and x-ray detectors. The emission direction from the sample surface can be freely selected for any orientation of the surface. For the surface preparation, the sample is translated in the preparation chamber [base pressure of $(1-2)\times10^{-10}$ mbar] equipped with facilities for sputtering, evaporation cells, gas inlets, and a reflection high-energy electron-diffraction (RHEED) system.

The surface preparation procedure was set up in previous He diffraction experiments.[23,24] The procedure takes into account the particular thermodynamics of $Cu_3Au(001)$, that is characterized by a continuous order/disorder (O/D) phase transition at the surface with a critical temperature[24] $T_c = 663$ K and a bulk first-order O/D transition at the same T_c.[25] An ordered surface, displaying sharp $c(2\times2)$ RHEED patterns typical of the Au-Cu termination,[26] was obtained by sputtering and careful annealing procedures described in details elsewhere.[24] The same sample was also used in a previous synchrotron experiment[20] and in the PDMEE experiment of Ref. 14.

At ALOISA, x-ray photoemission spectroscopy (XPS) surveys at grazing incidence (of the order of the critical angle) were used to check contamination of light adsorbates and Fe residuals after the sputtering removal of films. A preliminary ED characterization of the substrate, backed by multiple-scattering calculations has been presented in a previous paper.[20] Simulations taking into account the geometry for the Au-Cu termination available in literature[27] were found to be in excellent agreement with experimental results.

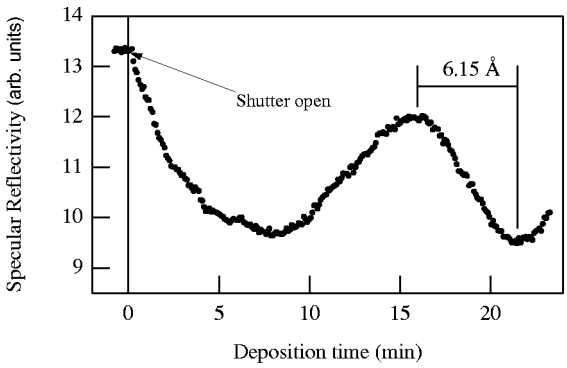

FIG. 1. x-ray specular reflectivity taken during deposition at fixed energy (3500 eV) and grazing angle (8.25°). Maxima and minima arise from the interference between the interface and the growing film surface.

Iron was evaporated from a carefully outgassed electron bombardment cell (Omicron). A quartz microbalance allowed to tune the deposition flux (typically of the order of one layer per minute) prior to the deposition on the sample. The quartz microbalance was calibrated by x-ray reflectivity from the sample during and after deposition. Figure 1 shows a typical deposition curve, measured at an incidence (tilt) angle $\alpha_{in}=8.25°$ and a photon energy of 3500 eV during film deposition at room temperature. The interference between the waves reflected by the film vacuum and the substrate-film interfaces yields an oscillatory evolution of the reflectivity as a function of the overlayer thickness. For the selected vertical momentum transfer $k_z=2(E/\hbar c)\sin\alpha_{in}$, identical phase conditions occur after a thickness increase of $\Delta D=2\pi/k_z=12.35$ Å, thus leading to an accurate calibration of the deposition rate.

The post growth GIXRD measurements consist of radial scans across the (200) and (220) peaks in the in-plane $Cu_3Au(001)$ reciprocal lattice. These measurements were taken scanning the photon energy in broad ranges under a suitable θ-2θ scattering geometry. The observation of diffraction peaks in radial scans allows to determine the in-plane spacing d through the Bragg condition $2d\sin\theta=hc/E$. Rocking curves of selected Bragg peaks, obtained by rotating the azimuthal angle at fixed energy, were measured to get additional information on the surface morphology.

A coverage estimate obtained by XPS measurements was found consistent with the reflectivity measurements within $\pm20\%$. ED polar scans were measured by rotating the electron analyzer in the plane defined by the surface normal and the beam axis, while keeping the grazing angle, the surface azimuthal orientation with respect to the beam axis and the polarization orientation fixed. We considered emission along the two main symmetry direction $\langle100\rangle_{sub}$ and $\langle110\rangle_{sub}$ of the substrate unit cell. The photon energy was set to about 900 eV in order to look at several photoelectron and Auger peaks of Fe, Cu, and Au. Here we will focus on the Fe $L_{2,3}M_{23}M_{45}$ line at a kinetic energy (KE) of 698 eV. The

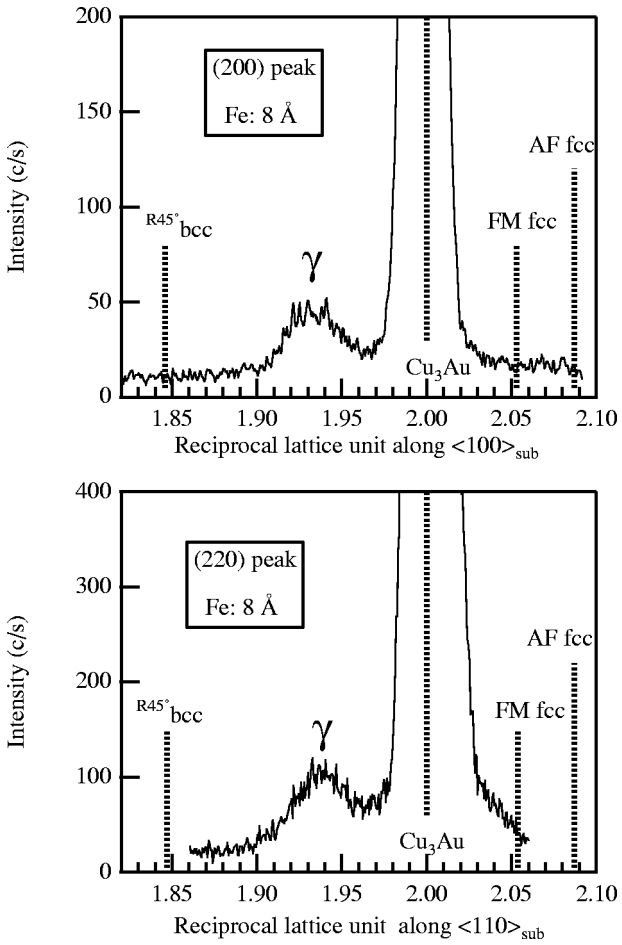

FIG. 2. In-plane x-ray diffraction of the (2,0,0), upper panel, and (2,2,0), lower panel, diffraction peaks taken at fixed scattering geometry by varying the photon energy. The photon beam impinges the surface at grazing incidence, forming an angle $\theta \sim 45°$ with respect to the fcc(100) planes of the direct lattice. The data are shown as a function of the $Cu_3Au(100)$ reciprocal-lattice unit in the corresponding lattice direction. Both diffraction patterns have been taken for the same Fe film at a thickness of ~ 8 Å. The vertical dotted lines correspond to the lattice of the antiferromagnetic (AF) and ferromagnetic (FM) fcc equilibrium structures as in Refs. 4 and 12; the bcc(100) lattice, rotated by 45° is also shown.

signal was collected at the maximum and at suitably chosen energies aside the peak, in order to allow an effective subtraction of the background of secondaries.

III. RESULTS

A. GIXRD

Radial scans of the substrate diffraction peaks, taken on films of different thickness, are expected to show additional diffraction features arising from the Fe overlayers, if the film unit cell, although strained, is oriented parallel to the substrate, as reported in the literature. Upon deposition at room temperature, the first Fe-induced peak arises at a thickness of ~ 8 Å. The radial scans across the (200) and (220) substrate peaks are shown in Fig. 2 as a function of the substrate reciprocal-lattice unit. The peaks labeled γ mark the appearance of a new structure, i.e., the overcome of the limit for pseudomorphic growth. The corresponding lattices for the antiferromagnetic and ferromagnetic fcc Fe are also shown for comparison,[4,12] as well as the lattice of a bcc(100) unit cell rotated by 45°. Azimuthal scans taken on the γ peaks (not shown) indicate this Fe phase to be oriented parallel to the substrate lattice.

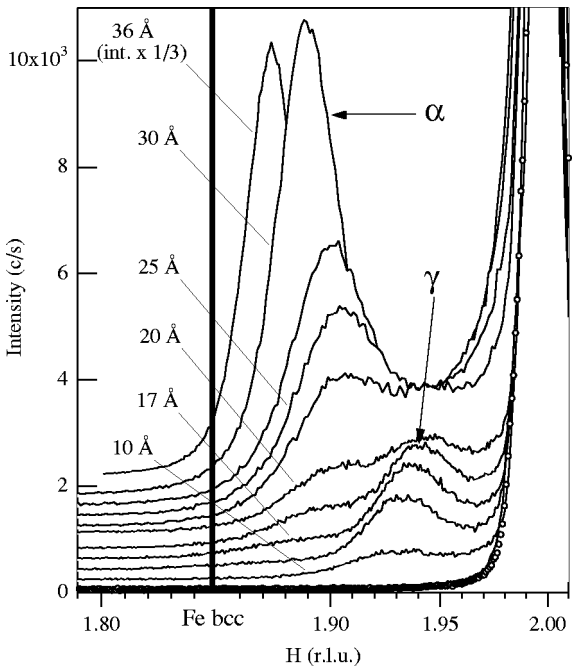

FIG. 3. In-plane x-ray diffraction of the (2,0,0) diffraction peak taken at fixed scattering geometry by varying the photon energy. The data are shown as a function of the reciprocal-lattice unit H of the fcc $Cu_3Au(100)$ substrate. Diffraction from the clean substrate is shown with open markers. Full lines are the diffraction measurements from Fe films at different thickness. The data have been vertically shifted by a constant offset (200 c/s) for the sake of clarity.

The evolution of the Fe film structure as the thickness increases is shown in Fig. 3, where radial scans across the (200) substrate peak are shown from 3 up to 36 Å. The peak γ becomes more intense in the (10–17)-Å range. A shoulder appears at the left-hand side of peak γ at $\Theta \geqslant 17$ Å. For $\Theta \geqslant 25$ Å this shoulder develops in the well-defined peak α, that gradually moves away from the (200) reflection.

The position 1.93 ± 0.005 reciprocal lattice unit (rlu) of the γ peak in the 10 Å pattern of Fig. 3, is the same of Fig. 2 at 8 Å and corresponds to a distance $d_{100} = 1.94 \pm 0.01$ Å along the $\langle 001 \rangle$ direction of direct space, eventually leading to a square cell of side $a_{\alpha'} = d\sqrt{2} = 2.74 \pm 0.01$ Å. The position of the α peak at 36 Å thickness in Fig. 3 corresponds to a lattice parameter $a_\alpha = 2.830 \pm 0.005$ Å. The position of α is indeed close to the (220) reflection of a ^{R45}bcc structure. Further, reasonable arguments on the energetics of iron modifications and inspection of the so-called epitaxial lines calculated in Ref. 4 led us to consider the α peak incompatible with an fcc-like modification [face-centered tetragonal phase (fct) phase]. The α peaks were therefore assigned to tetragonally strained body-centered (^{R45}bct) structures.

The GIXRD measurements provided therefore valuable insight on the in-plane structure of the films; this information is relatively direct for those patterns presenting one dominant Fe-induced peak, as it is the case at very low ($\leqslant 8$ Å) and very large coverages (36 Å). In an intermediate region between 10 and 20 Å, the patterns are more complex, likely reflecting the coexistence of more than one phase in the film. A full structural determination requires also the value of the vertical lattice constant of the various iron phases that forms at different thickness. We extracted this information by ED, in the forward focusing regime.

B. ED

ED polar scan measured on films of selected thickness for the Fe Auger line along the $\langle 100\rangle_{sub}$ and $\langle 110\rangle_{sub}$ directions, are reported in Figs. 4 and 5, respectively. The Fe films are the same of Fig. 3 at the corresponding thickness. The patterns were obtained after subtraction of the background of secondaries. The peak *F* is originated by the forward-scattering effect along off-normal nearest-neighbor chains. The position of this peak provides a guess on the ratio between the in-plane and vertical lattice constants of the film. In this respect, the full vertical lines in Figs. 4 and 5 mark the position of the *F* peak expected in case of fcc and ^{R45}bcc geometry, respectively.

At the lowest coverage investigated (patterns *a* of Figs. 4 and 5), the forward focusing peak *F* is fairly pronounced in the $\langle 100\rangle_{sub}$ scan close to the fcc-like position. The *F* peak lays close to the fcc marker in the $\langle 110\rangle_{sub}$ direction as well, though its intensity is very weak. Note in both patterns the presence of the forward focusing peak *N*, related to close-packed chains along the surface normal. At 10 Å (pattern *b* of Figs. 4 and 5) the *F* peaks move slightly from the fcc markers towards larger polar angles. The angular shift of the *F* peaks becomes more evident at $\Theta = 20$ Å (patterns *c*). Also the shape of the patterns shows evident variations with respect to lower coverages. In the spectra obtained on the film at $\Theta = 36$ Å (patterns *d*), the *F* peak becomes narrower and shifts towards the bcc position.

We performed also ED measurements for the Auger lines of Cu and for the Au $4f_{7/2}$ photoemission line. The experimental data resulted in overall agreement with results of Ref. 14, obtained on the same sample and under similar experimental conditions of this paper. We address the reader to Ref. 14 for a careful discussion of the intermixing between iron and substrate species.

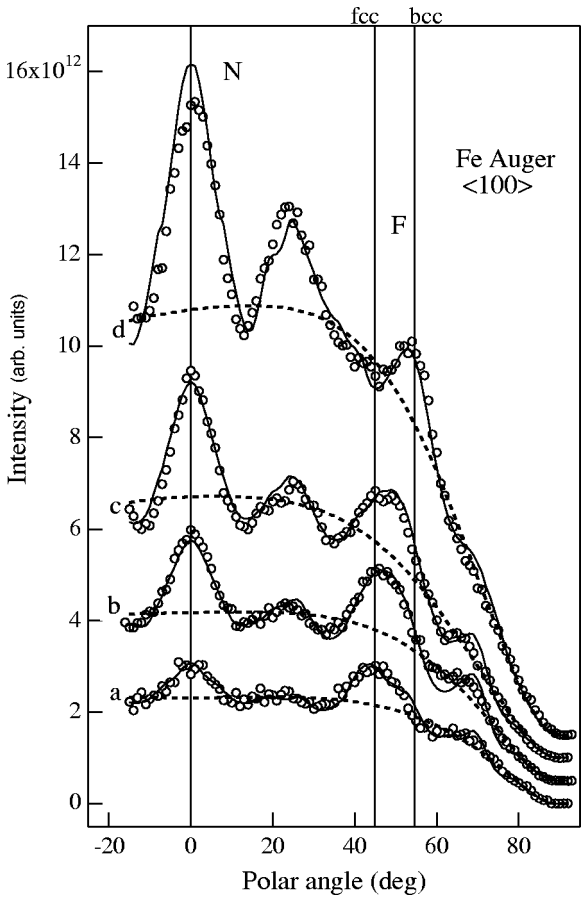

FIG. 4. Polar scans taken for the Fe Auger LMM (KE $= 698$ eV) peak along the $\langle 100\rangle$ substrate symmetry direction for: (a) the 3-Å film, (b) the 10-Å film, (c) the 20-Å film, (d) the 36-Å film. The polar scans are to scale and (b),(c),(d) have been vertically shifted by a constant offset for the sake of clarity. Full lines are the fits to the experimental ED data (open circles). The heavy dashed lines represent the ISO_{calc} components. The surface normal direction (*N*) and the first neighbor direction (*F*) are also indicated by the vertical full lines. (a) fit with a relaxed pseudomorphic phase ($a_p = 2.65$ Å, $c/a_p = 1.38$); (b) fit with a model that combines the relaxed pseudomorphic phase and the γ one (see text for the values of the lattice parameters and the weight of the phases); (c) fit with a linear combination of three phases (pseudomorphic, γ, and α), see text for the values of the lattice parameters and the weight of the phases; (d) fit with a body-centered tetragonal model structure ($a_\alpha = 2.83$ Å and $c/a_\alpha = 1.03$).

IV. ED DATA ANALYSIS

In this section we present the structural models for the Fe film at different thickness, as obtained by comparison of the ED experimental data to multiple-scattering calculations. In our computational approach the ED polar pattern $I_{exp}(\theta)$ is considered as a superposition of two contributions, according to the expression:

$$I_{exp}(\theta) = \mathrm{ISO}_{exp}(\theta)[1 + \chi_{exp}(\theta)], \qquad (1)$$

where $\mathrm{ISO}_{exp}(\theta)$ is a smooth, nearly isotropic background and the anisotropy term $\chi_{exp(\theta)}$ is the diffractive part of the pattern, carrying the information on the interatomic distances.

The ISO_{exp} contribution is commonly obtained by interpolating $I_{exp}(\theta)$ to a polynomial and divided out in order to extract χ_{exp}, which is then compared to calculated $\chi_{calc(\theta)}$.[28] We have preferred to afford a calculation of the ISO term. Thus, the polar scans $I_{exp}(\theta)$ have been compared with calculations

$$I_{calc}(\theta) = \mathrm{ISO}_{calc}(\theta)[1 + \chi_{calc}(\theta)]. \qquad (2)$$

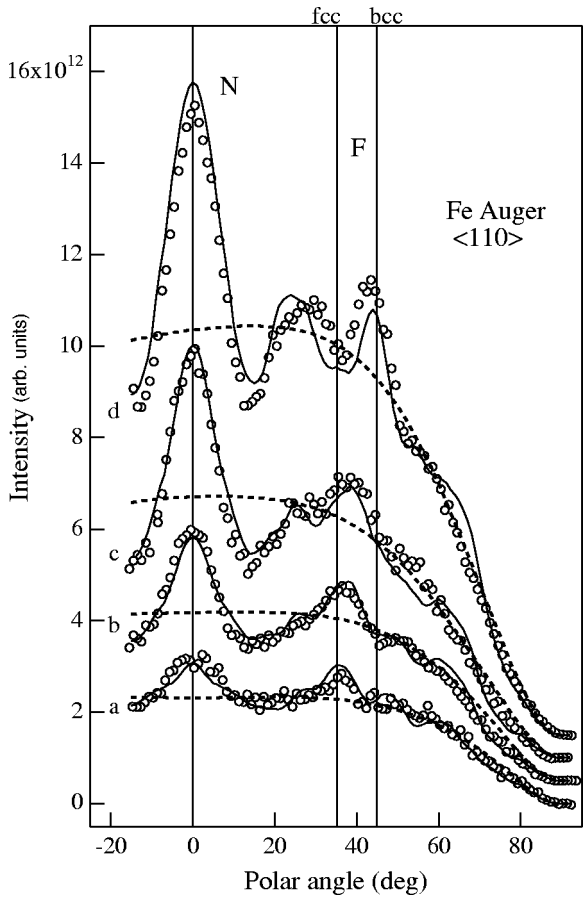

FIG. 5. Same of Fig. 4, but for the $\langle 110\rangle$ substrate symmetry direction for (a) the 3-Å film, (b) the 10-Å film, (c) the 20-Å film, (d) the 36-Å film. Full lines are the fits to the experimental ED data (open circles). The heavy dashed lines represent the ISO_{calc} component, which is the same for both azimuthal directions at the corresponding Fe thickness.

For any given model the anisotropy term χ_{calc} has been calculated by means of the MSCD code package,[29] while the ISO term has been written as the product of several factors.[30,31] First, an emission factor accounts for the electron emission matrix element;[32] it is determined by the polarization of the beam and by the initial and final states of the emitted electron. A second factor bears the information on the excited electron escape path through the Fe film;[30] it depends on the thickness and the homogeneity of the film. A third factor accounts for the surface roughness.[33] Final, an instrumental factor accounts for the beam-spot size on the sample and the angular acceptance of the detector. The calculation of the ISO part requires therefore reasonable estimates on the thickness and the surface roughness of the film and on the electronic mean free path.

Concerning MSCD calculations, the nonstructural input parameters, i.e., multiple-scattering order is 6 and the inner potential is 10 eV have been fixed for all the simulations. Clusters of at least 180 atoms have been considered. The isotropic emission for the Auger electrons has been simulated by the transition from an initial p level to an s $(l-1)$ final-state level.

The value of the lattice parameter of the in-plane square cell a has been obtained from the GIXRD measurement, while the ratio between the vertical spacing c and a , was first estimated by visual inspection of the angular position of the F peaks in the ED patterns. With these input parameters, the structural models have been refined by calculating $\chi_{calc(\theta)}$ as a function of a and c.

A. Low coverage: $\Theta < 8$ Å

The patterns of Figs. 4 and 5 force us to consider an fcc-like structure. Although results from Refs. 14 and 20 suggested a limited degree of mixing of Au in the first few layers, a reasonable fitting of the data was possible disregarding atomic exchange processes.[34] The comparison between MSCD calculations and the experimental ED scans is reported in Figs. 4 and 5 (curves labeled a). Note that the same $\mathrm{ISO}_{calc}(\theta)$ is used in both azimuthal directions.

The polar scans compare rather well with a simple three-layer Fe pseudomorphic fcc film ($a=2.65$ Å; $c/a=1.41$) built on an unrelaxed substrate extending three layers beneath. However, a slightly better agreement was found by admitting a slight tetragonal distortion with $a_p=2.65$ Å and $c/a_p=1.38$. The quality of the fit is observed to be slightly worst along the $\langle 110\rangle_{sub}$ direction. In fact, the ED polar scans are certainly affected by the film morphology[35] (such as preferred step orientation), but we cannot exclude a structural origin related to a very slight zigzag of the surface atom chains, which would smear the forward focusing features. In fact, a strong buckling was reported for the Fe on Cu(001) system,[36] where this distortion is predicted to be precursor of the fcc(100) to bcc(110) martensitic transition,[37] however, the latter transition is not observed on the present system.

B. Medium coverage: 8 Å$\leqslant\Theta\leqslant$20 Å

The γ peak in the GIXRD patterns at $\Theta\geqslant 8$ Å indicates a change of the growth mode. We first calculated the simulation for a homogeneous iron phase made of six complete layers, assuming the c/a ratio of 1.32 estimated by simple inspection of the angular position of the maximum of the F peak in the polar pattern. This model yields a simulation of the ED data (not shown) definitely not adequate. GIXRD and ED evidences can be rationalized if the coexistence of the two phases is assumed: the majority fcc-like phase, as seen at low coverage, is accompanied by the nucleation of a new phase γ, minority phase at this stage.

The ED patterns for the 10 Å Fe film thickness (curve b in Figs. 4 and 5) have been compared to calculations performed on a crude model assuming the linear combination of two ''independent'' phases:

$$I_{th}=AI_p+BI_\gamma, \tag{3}$$

where $I_p\rightarrow a_p=2.65$ Å and $c/a_p\sim 1.38$. $I_\gamma\rightarrow a_\gamma=2.74$ Å (from GIXRD) and c/a_γ to be determined. c/a_γ, A and B were varied in order to find the best agreement with experimental data.

Taking into account the estimated thickness of the film, we have modeled a film of about five to six layers. A good

agreement was obtained with $c/a_\gamma = 1.22$, $A = 0.6$, and $B = 0.4$ for both azimuthal directions (full line in polar scan *b* of Figs. 4 and 5).

For comparison, we also calculated the simulation for a homogeneous iron phase made of six complete layers, assuming the c/a ratio of 1.32 estimated by simple inspection of the angular position of the maximum of the *F* peak in the polar pattern. This model yields a simulation of the ED data (not shown) definitely worse than the mixed phases model.

At 20 Å the *F* peaks are clearly shifted, indicating a change of the c/a ratio. Backed by GIXRD, a model considering the superposition of three phases was attempted:

$$I_{th} = AI_p + BI_\gamma + CI_\alpha . \tag{4}$$

For simplicity, the parameters for the pseudomorphic and the γ phases were fixed at the same values found at lower coverage; $I_p \rightarrow a_p = 2.65$ Å, $c/a_p \sim 1.38$ and $I_\gamma \rightarrow a_\gamma = 2.74$ Å, $c/a_\gamma = 1.22$. By taking $A = 0.4$, $B = 0.4$, and $C = 0.2$, a rather satisfactory agreement was found (curves labeled *c* in Figs. 4 and 5) with the following set of parameters for the α phase:

$I_\alpha \rightarrow a_\alpha = 2.80$ Å, $c/a_\alpha = 1.05$.

We note that a reasonable agreement was found also with a linear combination of the pseudomorphic phase ($a_p = 2.65$ Å, $c/a_p \sim 1.38$) and the γ phase ($a_\gamma = 2.74$ Å, $c/a_\gamma = 1.22$) found at 10 Å. However, in this case, we have found rather different values of the *A* and *B* coefficients along the two azimuthal directions considered. Finally, the simulation for a homogeneous phase model assuming $c/a = 1.25$, corresponding to the angular position of the *F* peak in the polar scan, gave a bad quality fit.

C. High coverage: Θ>25 Å

The in-plane lattice parameter of the α phase at 36 Å determined by GIXRD is $a_\alpha = 2.830 \pm 0.005$ Å. The value of c/a_α was determined by simulation of scattering from a free-standing film consisting of a unique phase of 10 layers. The best fit yielded $a_\alpha = 2.83$ Å and $c/a_\alpha = 1.03 \pm 0.02$. The best-fit curves along $\langle 100 \rangle_{sub}$ and $\langle 110 \rangle_{sub}$ are reported in Figs. 4 and 5 (curves labeled *d*). We found an excellent agreement along the $\langle 100 \rangle_{sub}$ direction. The simulation reproduces rather accurately the angular position, intensity and width of the *N* and *F* peaks. The experimental data are not reproduced equally well along the $\langle 110 \rangle_{sub}$ direction, possibly due to some morphological effect.[35] A similar analysis, performed on the film of 30 Å thickness provided $a_\alpha = 2.810 \pm 0.005$ Å and $c/a_\alpha = 1.05 \pm 0.02$.

V. DISCUSSION

In Fig. 6, we report the comparison of our results and the other experimental data available in literature with the theoretical prediction for the structure of the bct and fct phases, the so-called epitaxial curves[4] (i.e., the curves where the Poisson ratio between the elastic constants for the given structure is conserved).

The single phase we found at the lower coverage represents the pseudomorphic phase predicted at initial stages of metal-on-metal epitaxy.[38] The occurrence of a pseudomorphic phase at low coverage is also reported by other measurements on $Cu_3Au(001)$ (Refs. 9 and 14) and $Cu_{90}Au_{10}(001)$.[39] As can be seen, this phase lies above the ferromagnetic (FM) fcc epitaxial line and is locked by the substrate for a few layers before the appearance of the γ phase at ~8 Å (for the pseudomorphic phase this thickness corresponds to 4.5 ML), which indicates that the limit for pseudomorphic growth has been overcome (in Fig. 6, we have reported the point at 10 Å for which the vertical spacing has been also determined by the ED analysis). These data are therefore consistent with the limit of 4 ML found in a recent experiment[14] and with the values obtained in earlier studies on this system.[3,8]

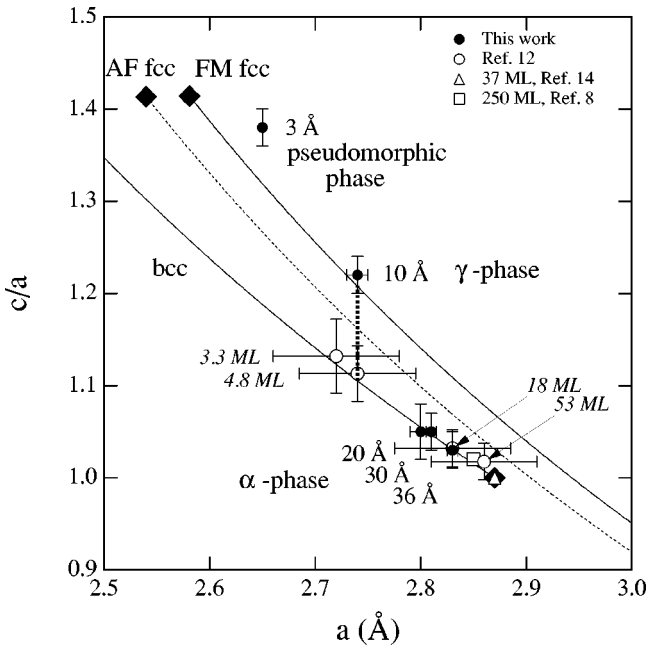

FIG. 6. Comparison of our results and other experimental data available in literature for thick films with the theoretical prediction for the structure of the bct [after Ref. 4] and fct [after Ref. 12] phases, the so-called epitaxial curves (full and dashed lines). The full circles represent our structural determinations, the thickness and corresponding Fe phase are indicated for each point. The open circles represent the determinations of Ref. 12, the corresponding thickness is also indicated (in italics). The open triangle and the open square represent the measurement of Ref. 14 at 37 ML and that of Ref. 8 for a 250-ML film, respectively. The path for the transition from the fct to bct phase is indicated by the heavy dotted line.

A relevant exception to such general agreement on initial stages of growth, is provided by the accurate analysis of Wuttig and co-workers.[10,12] As can be seen in Fig. 6, the films were found to lie on the bcc epitaxial line already at the coverage of 3.3 ML (i.e., ~5 Å, according to the data in Table I of Ref. 12). This discrepancy could be possibly attributed to the different procedure for film deposition, since the authors of Ref. 12 deposited the first two monolayers at 150 K, while subsequent layers were deposited at 300 K. This procedure is expected to reduce both intermixing and surface segregation. In fact, a fraction of the order of 10% of

a monolayer of Au atoms has been found to segregate for $\Theta < 4$ ML upon deposition at RT (Ref. 14) and a few percent has been found within the Fe film.[8,12,14] We may speculate that Au and Cu impurities are concurrent in the stabilization of the pseudomorphic phase. It is worth noting that a bcc-like structure has been recently suggested for (2–4)-ML Fe films on Cu(001), where segregation is certainly much lower.[40]

The morphology of the growing film is also affected by the deposition procedure. In fact, we previously found by He atom scattering that deposition of one layer equivalent at 150 K and subsequent annealing at 400 K yields the formation of an homogeneous pattern of three-layer height islands,[13] whereas a much higher filling of the first layer (68%) is obtained upon deposition of 1 ML at RT.[11]

Whatever the effect of temperature on segregation, structure, and morphology, our measurements do not support a direct relation between the SRO transition and the fct to bct one. In fact, the latter phase only appears at a thickness of 17 Å, i.e., well beyond the 2.5–3.5 ML range claimed in the literature for the SRO transition.[8–10] On the basis of the present data, we cannot exclude a connection between the transition from the pseudomorphic phase to the fct γ phase and the SRO transition.

The film evolution in the (10–20)-Å coverage range is the most interesting one since up to three different phases are seen to coexist. The γ phase is seen to fall on the epitaxial line for FM fcc Fe. Its lattice parameter at 8–10 Å, $a_\gamma = 2.74 \pm 0.01$ Å, seems to be the maximum allowed strain for this fct phase; in fact, when the third phase α appears at higher coverage, a_γ rather shrinks (see Fig. 3). This suggests that the appearance of the α phase partially relieves the strain of the fct film. The α phase, when appearing at 17 Å, has already a lateral lattice spacing of 2.80 Å, which, together with the vertical spacing determined by MSCD analysis, brings the new phase directly on the bcc epitaxial line. No diffraction features are observed for lateral lattice spacings ranging from 2.74 Å up to 2.80 Å. Upon further deposition, the ''asymptotic'' orthomorphic α phase evolves along the bcc epitaxial line. The structure of this phase is seen to be fully consistent with previous data reported in the literature for thick films.[8,12,14] From our data, the transition path between the fct and bct structure can be traced at the value of maximum tensile strain $a_\gamma = 2.74$ of the γ phase. The observation of a bct phase with the same lateral lattice constant was not possible, in fact the appearance of the α phase is accompanied by a partial relief of strain as witnessed by the slight decrease of a_γ, which corresponds to a volume decrease of the γ unit cell towards the predicted Fe fcc equilibrium point. On the other hand, the limit value for the bct stability was apparently reached by the group of Wuttig.[12] By following a different preparation procedure, they stabilized the bct phase down to four monolayers, with a corresponding lateral lattice constant in excellent agreement with the 2.74-Å value, we found for the limit of stability of the fct phase (see Fig. 6).

It is interesting to compare this system with the Fe/Cu(100) one. In the latter case, Fe is also seen to grow with an fcc pseudomorphic structure for at least 4 ML, at higher coverage the magnetic properties change and the formation of buffer layers with antiferromagnetic fcc structure is proposed. An fcc(100) to bcc(110) transition takes place at about 10 ML (which is also accompanied by an SRO transition) but, in this case, the whole film is observed to deconstruct, i.e., a martensitic phase transition takes place.[41,42] This is not observed for Fe on $Cu_3Au(001)$, where the γ phase is still detectable at a thickness of 20 Å. In any case the formation of the bct phase is accompanied by a significant amount of surface roughness, possibly leading to the exposure of the layers closer to the Fe/substrate interface (which are still probed by ED at 20 Å, see Sec. III B). This is consistent with a quantitative evaluation of the bct domain size obtained by the width of the diffracted α peaks. The profiles of the ^{R45}bct (110) and ^{R45}bct (100) peaks, obtained with an azimuthal scan at fixed photon energy (not shown), yielded a mean domain size of ~ 150 Å for the 36-Å film thickness. This high level of morphological disorder is consistent with the experimental findings for homoepitaxial deposition of Fe on Fe(001) at RT, where, in absence of surfactant species, the growth is seen to proceed in a three-dimensional fashion,[43,44] resulting in the formation of pyramidal moundlike structures.[45]

VI. CONCLUSIONS

We have presented a combined GIXRD-ED study of the growth of thin films of Fe on $Cu_3Au(001)$. We observed the formation of different phases as a function of the film thickness. The main conclusions of this investigation can be summarized as follows.

(1) A single pseudomorphic phase of nearly fcc character was observed below 8 Å thickness. This conclusion is consistent with most of the previous works in the literature[3,8,9,14] whereas it seems in apparent contrast with the analysis of Ref. 12 that reports a bct phase down to ~ 5 Å. In this respect, we suggested that exchange processes at the interface[14] may concur to the stabilization of the pseudomorphic phase and we speculate that the different results of Ref. 12 are due to a lower influence of intermixing obtained during the deposition of the first two layers at 150 K.

(2) On a 8-Å Fe thickness film, a neat Fe-induced peak, clearly illustrating the overcoming of the thickness limit for pseudomorphic growth, has been observed from the in-plane GIXRD measurements. Above this limit the film is characterized by the coexistence of phases: the pseudomorphic phase, most likely in inner layers, and a second strained phase γ. The latter phase is seen to lie on the ferromagnetic fcc epitaxial line.

(3) At $\theta \sim 17$ Å, we clearly observed the nucleation of a third strained phase, α, which becomes the dominating structure at $\theta \geqslant 25$ Å. The α phase is characterized by a body centered, tetragonally strained structure, whose unit cell is rotated by 45° with respect to the fcc substrate. The strain is progressively relieved with the increasing film thickness, in close agreement with the results of Ref. 12. The experimentally determined lattice constants of α are in strict quantitative agreement with the epitaxial curves for bcc Fe.

ACKNOWLEDGMENTS

Maurizio Canepa, Silvana Terreni, and Lorenzo Mattera are very grateful to Fernando Tommasini for his continuous support to this experiment. The authors are then grateful to P. Cantini, G. Boato, S. Valeri, and A. Di Bona for stimulating discussions on the Fe/Cu_3Au system. The authors thank G. Gazzadi for discussions on the MSCD calculations and C. Mannori and S. Prandi for helpful assistance at various stages of the experiment. Funding from INFM and from the Italian Ministero dell'Università e Ricerca Scientifica (Grant No. Cofin 990211848) are gratefully acknowledged.

*Corresponding author, FAX: **39-010-311066; Email address: canepa@fisica.unige.it; www.fisica.unige.it/surfmag

[1] M. Wuttig, B. Feldmann, and T. Flores, Surf. Sci. **331-333**, 659 (1995).

[2] V.L. Moruzzi, P.M. Marcus, and J. Kubler, Phys. Rev. B **39**, 6957 (1989); P.M. Marcus, V.L. Moruzzi, and S.L. Qiu, *ibid.* **60**, 369 (1999).

[3] S.H. Lu, J. Quinn, D. Tian, F. Jona, and P.M. Marcus, Surf. Sci. **209**, 364 (1989).

[4] P.M. Marcus and F. Jona, Surf. Rev. Lett. **1**, 15 (1994).

[5] D.D. Chambliss, R.J. Wilson, and S. Chiang, J. Vac. Sci. Technol. A **10**, 1993 (1992); M.T. Kief and W.F. Egelhoff, Phys. Rev. B **47**, 10 785 (1993).

[6] R. Opitz, S. Löbus, A. Thissen, and R. Courths, Surf. Sci. **370**, 293 (1997).

[7] O.S. Hernan, A.L. Vazquez de Parga, J.M. Gallego, and R. Miranda, Surf. Sci. **415**, 106 (1998).

[8] R. Rochow, C. Carbone, Th. Dodt, F.P. Johnen, and E. Kisker, Phys. Rev. B **41**, 3426 (1990).

[9] M.-T. Lin, J. Shen, W. Kuch, H. Jenniches, M. Klaua, C.M. Schneider, and J. Kirschner, Phys. Rev. B **55**, 5886 (1997).

[10] B. Feldmann, B. Schirmer, A. Sokoll, and M. Wuttig, Phys. Rev. B **57**, 1014 (1998).

[11] M.-T. Lin, J. Shen, W. Kuch, H. Jenniches, M. Klaua, C.M. Schneider, and J. Kirschner, Surf. Sci. **410**, 298 (1998).

[12] B. Schirmer, B. Feldmann, and M. Wuttig, Phys. Rev. B **58**, 4984 (1998).

[13] M. Canepa, P. Cantini, C. Mannori, S. Terreni, and L. Mattera, Phys. Rev. B **62**, 13 121 (2000); A. Verdini, L. Floreano, F. Bruno, D. Cvetko, A. Morgante, F. Bisio, S. Terreni, and M. Canepa, Phys. Rev. B **65**, 233403 (2002).

[14] P. Luches, A. Di Bona, S. Valeri, and M. Canepa, Surf. Sci. **471**, 32 (2000).

[15] An updated presentation of the beamline can be found at http: //www.tasc.infm.it/ tasc/ lds/ aloisa/ aloisa.html

[16] S. Kono, S.M. Goldberg, N.F.T. Hall, and C.S. Fadley, Phys. Rev. Lett. **41**, 1831 (1978).

[17] C. S. Fadley, *The Study of Surface Structures by Photoelectron Diffraction and Auger Electron Diffraction* in *Synchrotron Radiation research: Advances in Surface and Interface Science, Vol. 1: Techniques*, edited by R. Z. Bachrach (Plenum, New York, 1992), and references therein.

[18] W. F. Egelhoff, Jr., in *Ultrathin Magnetic Structures I*, edited by J. A. C. Bland and B. Heinrich (Springer-Verlag, Berlin, 1994), Chap. 5.1, p. 220.

[19] Y. Chen, F.J. Garcia de Abajo, A. Chassé, R.X. Ynzunza, A.P. Kaduwela, M.A. Van Hove, and C.S. Fadley, Phys. Rev. B **58**, 13 121 (1998).

[20] F. Bruno, D. Cvetko, L. Floreano, R. Gotter, C. Mannori, L. Mattera, R. Moroni, S. Prandi, S. Terreni, A. Verdini, and M. Canepa, Appl. Surf. Sci. **162-163**, 340 (2000).

[21] B.M. Lairson, A.P. Payne, S. Brennan, N.M. Rensing, B.J. Daniels, and B.M. Clemens, J. Appl. Phys. **78**, 4449 (1995).

[22] L. Floreano, G. Naletto, D. Cvetko, R. Gotter, M. Malvezzi, L. Marassi, A. Morgante, A. Santaniello, A. Verdini, F. Tommasini, and G. Tondello Rev. Sci. Instrum. **70**, 3855 (1999).

[23] C. Mannori, T. Scimia, P. Cantini, S. Terreni, M. Canepa, and L. Mattera, Surf. Sci. **433**, 307 (1999).

[24] C. Mannori, G. Boato, M. Canepa, P. Cantini, L. Mattera, and S. Terreni, Europhys. Lett. **45**, 686 (1999).

[25] For a review, see H. Dosch, *Critical Phenomena at surfaces and interfaces*, edited by G. Höhler, Springer Tracts Mod. Phys. Vol. 126 (Springer, Berlin, 1992).

[26] E.G. McRae and R. Malic, Surf. Sci. **148**, 551 (1984).

[27] W.E. Wallace and G.J. Auckland, Surf. Sci. Lett. **275**, L685 (1992).

[28] G.C. Gazzadi, P. Luches, A. di Bona, L. Marassi, L. Pasquali, S. Valeri, and S. Nannarone, Phys. Rev. B **61**, 2246 (2000).

[29] http://electron.lbl.gov/mscdpack/mscdpack.html. Further information can be found in MSCD *Package User Guide - Simulation of Photoelectron Diffraction using Rehr-Albers Separable Representation*, by Y. Chen and M. A. Van Hove, handed out at Trieste School on Use of Synchrotron Radiation, 1997.

[30] C. S. Fadley, *Basics Concepts of X-Ray Photoelectron Spectroscopy* in *Electron Spectroscopy, Theory, Techniques and Applications*, edited by C. R. Brundle and A. D. Baker (Pergamon, New York, 1978), Vol. II, Chap. 1.

[31] F. Bruno, L. Floreano, A. Verdini, D. Cvetko, R. Gotter, A. Morgante, M. Canepa, and S.Terreni, in press, cond-mat/0204404, J. Elecron Spectrosc. Relat. Phenom (to be published).

[32] J.W. Cooper, Phys. Rev. A **47**, 1841 (1993).

[33] A.V. Yakovenko, J. Electron Spectrosc. Relat. Phenom. **74**, 237 (1995).

[34] The substrate temperature proved to be a very critical parameter in determining the level of Au surface segregation. In fact, the higher Au concentration at the Fe film surface, we found in the preliminary experiments [Ref. 20], was associated with a slightly higher (15–20 °C) substrate temperature during deposition.

[35] Y. Park, E.E. Fullerton, and S.D. Bader, Appl. Phys. Lett. **66**, 2140 (1995).

[36] S. Müller, P. Bayer, C. Reischl, K. Heinz, B. Feldmann, H. Zillgen, and M. Wuttig, Phys. Rev. Lett. **74**, 765 (1995).

[37] D. Spisak and J. Hafner, Phys. Rev. Lett. **88**, 056101 (2002).

[38] J.H. Van Der Merwe, J. Appl. Phys. **34**, 117 (1963).

[39] S.S. Kang, W. Kuch, and J. Kirschner, Phys. Rev. B **63**, 024401 (2000).

[40] A. Biedermann, R. Tscheließnig, M. Schmid, and P. Varga, Phys. Rev. Lett. **87**, 086103 (2001).

[41] K. Kalki, D.D. Chambliss, K.E. Johnson, R.J. Wilson, and S.

Chiang, Phys. Rev. B **48**, 18 344 (1993); S. Müller, P. Bayer, C. Reischl, K. Heinz, B. Feldmann, H. Zillgen, and M. Wuttig, Phys. Rev. Lett. **74**, 765 (1995); J. Giergiel, J. Shen, J. Wolterstorf, A. Kirilyuk, and J. Kirschner, Phys. Rev. B **52**, 8528 (1995).

[42] A. Biedermann, M. Schmid, and P. Varga, Phys. Rev. Lett. **86**, 464 (2001).

[43] J.A. Stroscio, D.T. Pierce, and R.A. Dragoset, Phys. Rev. Lett. **70**, 3615 (1993).

[44] P. Bonanno, M. Canepa, P. Cantini, L. Mattera, R. Moroni, and S. Terreni, Surf. Sci. **454-456**, 697 (2000).

[45] K. Thürmer, R. Koch, M. Weber, and K.H. Rieder, Phys. Rev. Lett. **75**, 1767 (1995).